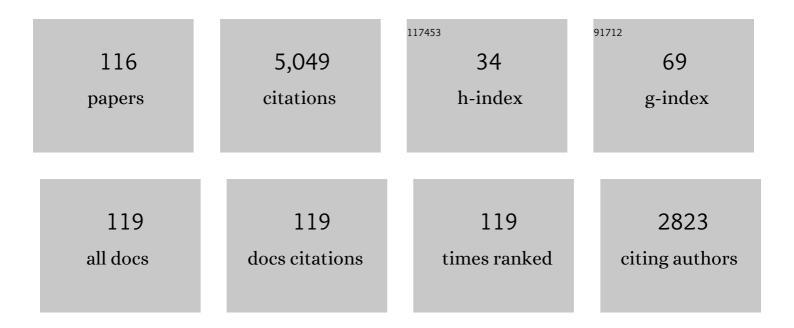
List of Publications by Year in descending order

Source: https://exaly.com/author-pdf/942409/publications.pdf Version: 2024-02-01



**RINTARO LIFU** 

#	Article	IF	CITATIONS
1	Preferable Resistance against Hydrogen Embrittlement of Pearlitic Steel Deformed by Caliber Rolling. ISIJ International, 2022, 62, 368-376.	0.6	4
2	True Stress–True Strain Relationship up to the Plastic Deformation Limit in Ferrite–Pearlite Steel at Various Temperatures. ISIJ International, 2022, 62, 361-367.	0.6	0
3	Deformation behaviour of novel medium carbon bainitic steels with different retained austenite characteristics designed by the sparse mixed regression model. Journal of Materials Research and Technology, 2022, 19, 2179-2190.	2.6	2
4	Effect of strain and deformation mode on cube texture formation in warm bi-axial rolled low-carbon steel. Finite Elements in Analysis and Design, 2021, 183-184, 103491.	1.7	1
5	Crystallographic orientation dependence of deformation-induced martensitic transformation of 1.3 GPa-class 0.6 %C bainitic steel with retained austenite. Scripta Materialia, 2021, 194, 113666.	2.6	5
6	Effect of Temperature on Stress–Strain Curve in SUS316L Metastable Austenitic Stainless Steel studied by <i>In Situ</i> Neutron Diffraction Experiments. Tetsu-To-Hagane/Journal of the Iron and Steel Institute of Japan, 2021, 107, 741-750.	0.1	0
7	Bainite Transformation and Resultant Tensile Properties of 0.6%C Low Alloyed Steels with Different Prior Austenite Grain Sizes. ISIJ International, 2021, 61, 582-590.	0.6	11
8	Effect of Temperature on Stress–Strain Curve in SUS316L Metastable Austenitic Stainless Steel Studied by <i>In Situ</i> Neutron Diffraction Experiments. ISIJ International, 2021, 61, 632-640.	0.6	5
9	Ductile-to-Brittle Transition and Brittle Fracture Stress of Ultrafine-Grained Low-Carbon Steel. Materials, 2021, 14, 1634.	1.3	20
10	Grain-to-Grain Interaction Effect in Polycrystalline Plain Low-Carbon Steel within Elastic Deformation Region. Materials, 2021, 14, 1865.	1.3	1
11	Plastic Instability in Medium-Carbon Tempered Martensite Steel. Materials, 2021, 14, 4609.	1.3	1
12	In-Situ Observation of Lüders Band Formation in Hot-Rolled Steel via Digital Image Correlation. Metals, 2020, 10, 530.	1.0	12
13	Improvement of strength, toughness and ductility in ultrafine-grained low-carbon steel processed by warm bi-axial rolling. Materials Science & Engineering A: Structural Materials: Properties, Microstructure and Processing, 2020, 786, 139415.	2.6	24
14	Experimental measurement of the variables of Lüders deformation in hot-rolled steel via digital image correlation. Materials Science & Engineering A: Structural Materials: Properties, Microstructure and Processing, 2020, 790, 139756.	2.6	14
15	Heterogeneous Distribution of Microstrain Evolved During Tensile Deformation of Polycrystalline Plain Low Carbon Steel. Metals, 2020, 10, 774.	1.0	6
16	Through-Thickness Microstructure and Strain Distribution in Steel Sheets Rolled in a Large-Diameter Rolling Process. Metals, 2020, 10, 91.	1.0	7
17	Acceleration of diffusional transformation in a high-carbon steel layer composed of a sandwich-like clad steel sheet. Materials Science & Engineering A: Structural Materials: Properties, Microstructure and Processing, 2019, 764, 138217.	2.6	2
18	Formation Mechanism of Ultrafine Grained Microstructures: Various Possibilities for Fabricating Bulk Nanostructured Metals and Alloys. Materials Transactions, 2019, 60, 1518-1532.	0.4	34

#	Article	IF	CITATIONS
19	Acceleration of pearlite transformation in a high-carbon steel by uniaxial compressive stress confirmed by volume measurements. Materials Letters, 2019, 256, 126637.	1.3	3
20	Effect of Interface Morphology on Tensile Properties of Carbon Steel Sheet with Sandwich Structure. Steel Research International, 2019, 90, 1900015.	1.0	1
21	Improvement of toughness and strength balance in low-carbon steel bars with cube texture processed by warm bi-axial rolling. Materials Letters, 2019, 240, 172-175.	1.3	8
22	Optimization of microstructure at Ni-C steel joint by friction stir welding with CO2 cooling. Welding International, 2018, 32, 338-344.	0.3	8
23	Fatigue strength of hot-stamped spot welded joints*—study on spot welding tailored blank technology. Welding International, 2018, 32, 264-273.	0.3	1
24	Study on static and fatigue strength of structural adhesive-bonded joints of steel sheets for automotive application. Welding International, 2018, 32, 353-362.	0.3	3
25	Static strength of hot-stamped spot welded joints: study on spot welding tailored blank technology. Welding International, 2017, 31, 681-691.	0.3	4
26	Strain-Rate and Temperature Dependences of Deformation Behavior of AZ61Mg Alloy Processed by Multi-directional Forging Under Decreasing Temperature Conditions. Metallurgical and Materials Transactions A: Physical Metallurgy and Materials Science, 2017, 48, 5368-5375.	1.1	5
27	Effect of Layer Construction on Tensile Deformation Behavior of Japanese-Sword-Type Steel Sheet. Journal of the Japan Society for Technology of Plasticity, 2017, 58, 323-329.	0.0	1
28	Strength and Ductility at High-speed Tensile Deformation of Low-carbon Steel with Ultrafine Grains. Materials Transactions, 2017, 58, 1487-1492.	0.4	1
29	Study on static and fatigue strength of structural adhesive bonded joints of steel sheets for automotive application. Yosetsu Gakkai Ronbunshu/Quarterly Journal of the Japan Welding Society, 2016, 34, 93-101.	0.1	1
30	Improvement of Fatigue Properties of Resistance Spot Welded Joints in High Strength Steel Sheets by Shot Blast Processing. ISIJ International, 2016, 56, 1276-1284.	0.6	10
31	Stability of the retained austenite in low-alloyed transformation induced plasticity-aided steels during friction stir welding. Science and Technology of Welding and Joining, 2016, 21, 281-286.	1.5	11
32	Phase transformation in Fe–Mn–C alloys by severe plastic deformation under high pressure. Materials Letters, 2016, 185, 109-111.	1.3	3
33	Dynamic and static change of grain size and texture of copper during friction stir welding. Journal of Materials Processing Technology, 2016, 232, 90-99.	3.1	42
34	Investigation into feasibility of FSW process for welding 1600 MPa quenched and tempered steel. Materials Science & Engineering A: Structural Materials: Properties, Microstructure and Processing, 2016, 651, 904-913.	2.6	45
35	Stabilization of austenite in low carbon Cr–Mo steel by high speed deformation during friction stir welding. Materials and Design, 2016, 90, 915-921.	3.3	27
36	Effect of online rapid cooling on microstructure and mechanical properties of friction stir welded medium carbon steel. Journal of Materials Processing Technology, 2016, 230, 62-71.	3.1	37

#	Article	IF	CITATIONS
37	Microstructure and texture distribution of Ti–6Al–4V alloy joints friction stir welded below β-transus temperature. Journal of Materials Processing Technology, 2016, 229, 390-397.	3.1	53
38	Effect of initial grain size on inhomogeneous plastic deformation and twinning behavior in high manganese austenitic steel with a polycrystalline microstructure. IOP Conference Series: Materials Science and Engineering, 2015, 89, 012045.	0.3	6
39	Fatigue strength of hot-stamped spot welded joints. Yosetsu Gakkai Ronbunshu/Quarterly Journal of the Japan Welding Society, 2015, 33, 253-261.	0.1	5
40	Optimization of Microstructure at Ni-C steel joint by friction stir welding with CO <sub>2</sub> cooling. Yosetsu Gakkai Ronbunshu/Quarterly Journal of the Japan Welding Society, 2015, 33, 358-364.	0.1	1
41	Static strength of hot-stamped spot welded joints. Yosetsu Gakkai Ronbunshu/Quarterly Journal of the Japan Welding Society, 2015, 33, 144-152.	0.1	10
42	Development of small sized friction stir welding equipment for hand operated welding. Science and Technology of Welding and Joining, 2015, 20, 249-253.	1.5	4
43	Effect of rotation rate on microstructure and texture evolution during friction stir welding of Ti–6Al–4V plates. Materials Characterization, 2015, 106, 352-358.	1.9	61
44	Double-sided friction-stir welding of magnesium alloy with concave–convex tools for texture control. Materials & Design, 2015, 76, 181-189.	5.1	49
45	Microstructural control and mechanical properties in friction stir welding of medium carbon low alloy S45C steel. Materials Science & Engineering A: Structural Materials: Properties, Microstructure and Processing, 2015, 636, 24-34.	2.6	38
46	Effect of initial microstructure on Ti–6Al–4V joint by friction stir welding. Materials and Design, 2015, 88, 1269-1276.	3.3	52
47	Enhanced mechanical properties of 70/30 brass joint by multi-pass friction stir welding with rapid cooling. Science and Technology of Welding and Joining, 2015, 20, 91-99.	1.5	26
48	Mechanical properties of advanced active-TIG welded duplex stainless steel and ferrite steel. Materials Science & Engineering A: Structural Materials: Properties, Microstructure and Processing, 2015, 620, 140-148.	2.6	21
49	Enhanced tensile properties of Fe–Ni–C steel resulting from stabilization of austenite by friction stir welding. Journal of Materials Processing Technology, 2015, 216, 216-222.	3.1	44
50	Stabilization of the Retained Austenite in Steel by Friction Stir Welding. , 2015, , 47-54.		2
51	Development of Small sized Friction Stir Welding Equipment for Hand-operated Welding. Yosetsu Gakkai Ronbunshu/Quarterly Journal of the Japan Welding Society, 2014, 32, 52-56.	0.1	Ο
52	Effect of oxygen on weld shape and crystallographic orientation of duplex stainless steel weld using advanced A-TIG (AA-TIG) welding method. Materials Characterization, 2014, 91, 42-49.	1.9	35
53	Enhanced mechanical properties in friction stir welded low alloy steel joints via structure refining. Materials Science & Engineering A: Structural Materials: Properties, Microstructure and Processing, 2014, 606, 322-329.	2.6	28
54	High strength and ductility of friction-stir-welded steel joints due to mechanically stabilized metastable austenite. Scripta Materialia, 2014, 70, 39-42.	2.6	56

#	Article	IF	CITATIONS
55	Increase of bending fatigue resistance for tungsten inert gas welded SS400 steel plates using friction stir processing. Materials & Design, 2014, 61, 275-280.	5.1	24
56	Modification of mechanical properties of friction stir welded Cu joint by additional liquid CO2 cooling. Materials & Design, 2014, 56, 20-25.	5.1	62
57	Enhanced mechanical properties of 70/30 brass joint by rapid cooling friction stir welding. Materials Science & Engineering A: Structural Materials: Properties, Microstructure and Processing, 2014, 610, 132-138.	2.6	64
58	Friction powder compaction process for fabricating open-celled Cu foam by sintering-dissolution process route using NaCl space holder. Materials Science & Engineering A: Structural Materials: Properties, Microstructure and Processing, 2013, 585, 468-474.	2.6	42
59	Fine grained Mg–3Al–1Zn alloy with randomized texture in the double-sided friction stir welded joints. Materials Science & Engineering A: Structural Materials: Properties, Microstructure and Processing, 2013, 580, 83-91.	2.6	71
60	Role of stress-induced martensitic transformation in TRIP effect of metastable austenitic steels. Journal of Alloys and Compounds, 2013, 577, S525-S527.	2.8	8
61	Fully recrystallized nanostructure fabricated without severe plastic deformation in high-Mn austenitic steel. Scripta Materialia, 2013, 68, 813-816.	2.6	112
62	Crystallographic orientation dependence of ε martensite transformation during tensile deformation of polycrystalline 30% Mn austenitic steel. Materials Science & Engineering A: Structural Materials: Properties, Microstructure and Processing, 2013, 576, 14-20.	2.6	34
63	Improvement of toughness and strength of thick structural steel weld by friction stir welding conditions. Science and Technology of Welding and Joining, 2013, 18, 287-292.	1.5	8
64	Effects of Temperature and Strain Rate on TRIP Effect in SUS301L Metastable Austenitic Stainless Steel. ISIJ International, 2013, 53, 1881-1887.	0.6	47
65	Grain size effect on high-speed deformation of Hadfield steel. Journal of Materials Science, 2012, 47, 7946-7953.	1.7	15
66	Microstructures and mechanical properties evolution during friction stir welding of SK4 high carbon steel alloy. Materials Science & Engineering A: Structural Materials: Properties, Microstructure and Processing, 2012, 558, 572-578.	2.6	38
67	Numerical Homogenization Methods Based on Heterogeneous Microstructure in Multi-Constituent Steels. Tetsu-To-Hagane/Journal of the Iron and Steel Institute of Japan, 2012, 98, 283-289.	0.1	5
68	Effect of Grain Size and Grain Orientation on Dislocations Structure in Tensile Strained TWIP Steel During Initial Stages of Deformation. Steel Research International, 2012, 83, 374-378.	1.0	16
69	Pressure-induced Phase Transformation Behavior in ^ ^alpha;-Mn Steels by High-pressure Torsion Straining. Tetsu-To-Hagane/Journal of the Iron and Steel Institute of Japan, 2012, 98, 541-547.	0.1	1
70	OS0115 Ductility of Hadfield steel at high speed or warm temperature deformation. The Proceedings of the Materials and Mechanics Conference, 2012, 2012, _OS0115-1OS0115-2	0.0	0
71	Influence of Strain Rate on TRIP Effect in SUS301L Metastable Austenite Steel. Tetsu-To-Hagane/Journal of the Iron and Steel Institute of Japan, 2011, 97, 450-456.	0.1	18
72	Stress-Induced Martensitic Transformation Behaviors at Various Temperatures and Their TRIP Effects in SUS304 Metastable Austenitic Stainless Steel. ISIJ International, 2011, 51, 124-129.	0.6	97

#	Article	IF	CITATIONS
73	Deformation behavior of pure titanium at a wide range of strain rates. Journal of Physics: Conference Series, 2010, 240, 012021.	0.3	4
74	Mechanical properties of 15%Mn steel with fine lamellar structure consisting of ferrite and austenite phases. Journal of Physics: Conference Series, 2010, 240, 012029.	0.3	0
75	Effect of Cementite Volume Fraction on Static Tensile Properties in Ultrafine-grained Ferrite–Cementite Steels. Tetsu-To-Hagane/Journal of the Iron and Steel Institute of Japan, 2010, 96, 42-50.	0.1	8
76	Improved tensile properties of partially recrystallized submicron grained TWIP steel. Materials Letters, 2010, 64, 15-18.	1.3	114
77	Friction stir welding of high carbon steel with excellent toughness and ductility. Scripta Materialia, 2010, 63, 223-226.	2.6	123
78	Flow stress analysis of TWIP steel via the XRD measurement of dislocation density. Materials Science & Engineering A: Structural Materials: Properties, Microstructure and Processing, 2010, 527, 2759-2763.	2.6	265
79	Tensile deformation behavior of high manganese austenitic steel: The role of grain size. Materials & Design, 2010, 31, 3395-3402.	5.1	198
80	Effect of Si Content on Fracture Behaviour Change by Strain Rate in Si Steels. Materials Science Forum, 2010, 654-656, 1303-1306.	0.3	6
81	Grain Size Dependence of the Flow Stress of TWIP Steel. Materials Science Forum, 2010, 654-656, 294-297.	0.3	11
82	Grain Size Effect on the Martensite Formation in a High-Manganese TWIP Steel by the Rietveld Method. Journal of Materials Science and Technology, 2010, 26, 181-186.	5.6	61
83	Morphology-Change of Mg_2Si and Strength-Change in Boron-Added Al-Mg-Si Alloys. Nihon Kikai Gakkai Ronbunshu, A Hen/Transactions of the Japan Society of Mechanical Engineers, Part A, 2009, 75, 896-900.	0.2	1
84	Enantiomorph identification and stacking faults in κ-(BEDT-TTF)2Cu(NCS)2by convergent-beam electron diffraction. Journal of Applied Crystallography, 2009, 42, 433-441.	1.9	2
85	Friction stir welding of hypereutectoid steel (SK5) below eutectoid temperature. Science and Technology of Welding and Joining, 2009, 14, 233-238.	1.5	39
86	Tensile properties and twinning behavior of high manganese austenitic steel with fine-grained structure. Scripta Materialia, 2008, 59, 963-966.	2.6	377
87	Relations between Dewetting of Polymer Thin Films and Phase-Separation of Encompassed Quantum Dots. Journal of Physical Chemistry C, 2008, 112, 8184-8191.	1.5	22
88	Managing Both Strength and Ductility in Ultrafine Grained Steels. ISIJ International, 2008, 48, 1114-1121.	0.6	126
89	Role of Stress-Induced Martensitic Transformation in TRIP Effect of Metastable Austenitic Stainless Steels. Nippon Kinzoku Gakkaishi/Journal of the Japan Institute of Metals, 2008, 72, 769-775.	0.2	23
90	Effects of Carbon and Silicon on Static/Dynamic Mechanical Properties of 780 MPa Grade Dual Phase Steel. Tetsu-To-Hagane/Journal of the Iron and Steel Institute of Japan, 2008, 94, 305-312.	0.1	6

#	Article	IF	CITATIONS
91	Effect of Grain Size on Tensile Properties of TWIP Steel. Nippon Kinzoku Gakkaishi/Journal of the Japan Institute of Metals, 2007, 71, 815-821.	0.2	23
92	Effect of Niobium or Vanadium on Mechanical Properties of Hot Rolled High Strength Steel Sheets for Automotive Use. Tetsu-To-Hagane/Journal of the Iron and Steel Institute of Japan, 2007, 93, 451-458.	0.1	2
93	Structural and optical studies of (AlAs)m/(GaAs)n type-I ultra short-period superlattices with fractional monolayer. Journal of Crystal Growth, 2007, 301-302, 168-171.	0.7	1
94	GaNAs/GaAs multiple quantum well grown by modulated N radical beam sequence of RF-MBE: Effect of growth interruption. Journal of Crystal Growth, 2007, 301-302, 583-587.	0.7	5
95	Effects of the Grain Size and Volume Fraction of Second Hard Phase on Mechanical Properties of Dual Phase Steel. Tetsu-To-Hagane/Journal of the Iron and Steel Institute of Japan, 2006, 92, 457-463.	0.1	20
96	Friction Stir Welding of Ultrafine Grained Interstitial Free Steels. Materials Transactions, 2006, 47, 239-242.	0.4	87
97	Crystallographic features of lath martensite in low-carbon steel. Acta Materialia, 2006, 54, 1279-1288.	3.8	781
98	Friction stir welding of ultrafine grained plain low-carbon steel formed by the martensite process. Materials Science & Engineering A: Structural Materials: Properties, Microstructure and Processing, 2006, 423, 324-330.	2.6	115
99	Fabrication of a quantum dot-polymer matrix by layer-by-layer conjugation. Journal of Photochemistry and Photobiology A: Chemistry, 2006, 183, 285-291.	2.0	21
100	Internal Stress Field in Ultrafine Grained Aluminium Fabricated by Accumulative Roll-Bonding. Materials Science Forum, 2006, 512, 123-128.	0.3	1
101	Structural Analyses of Fractional Monolayer (GaAs)m/(AlAs)nSuperlattices by X-ray Resonant/Off-Resonant Scattering. Japanese Journal of Applied Physics, 2006, 45, 3548-3551.	0.8	6
102	Crystallographic analysis of plate martensite in Fe–28.5 at.% Ni by FE-SEM/EBSD. Materials Characterization, 2005, 54, 378-386.	1.9	146
103	Measurement of Internal Stress in Ultrafine Grained Aluminium by CBED. Materia Japan, 2005, 44, 985-985.	0.1	0
104	Crystallographic Features of Lath Martensite in 0.20%C Steel Analyzed by FE-SEM/EBSD. Materia Japan, 2005, 44, 982-982.	0.1	0
105	Structure and strength after large strain deformation. Materials Science & Engineering A: Structural Materials: Properties, Microstructure and Processing, 2004, 387-389, 191-194.	2.6	92
106	Effect of rolling reduction on ultrafine grained structure and mechanical properties of low-carbon steel thermomechanically processed from martensite starting structure. Science and Technology of Advanced Materials, 2004, 5, 153-162.	2.8	100
107	A new and simple process to obtain nano-structured bulk low-carbon steel with superior mechanical property. Scripta Materialia, 2002, 46, 305-310.	2.6	237
108	Nanoscale crystallographic analysis of ultrafine grained IF steel fabricated by ARB process. Scripta Materialia, 2002, 47, 69-76.	2.6	141

#	Article	IF	CITATIONS
109	Ultragrain refinement of plain low carbon steel by cold-rolling and annealing of martensite. Acta Materialia, 2002, 50, 4177-4189.	3.8	322
110	Ultra-Fine Grains in Ultra Low Carbon IF Steel Highly Strained by ARB. Materia Japan, 2000, 39, 961-961.	0.1	15
111	High Speed Deformation of Ultrafine Grained TWIP Steel. Materials Science Forum, 0, 561-565, 107-110.	0.3	19
112	Strain Rate Sensitivity of 31Mn-3Al-3Si TWIP Steel with Partially Recrystallized Fine Grained Structure. Materials Science Forum, 0, 584-586, 673-678.	0.3	7
113	High Cycle Fatigue Behavior of Cold Forging Die Steel. Key Engineering Materials, 0, 417-418, 225-228.	0.4	5
114	Fracture Behavior Transition by Change of Strain Rate in Dislocation-Induced Si Steels. Materials Science Forum, 0, 706-709, 2187-2192.	0.3	2
115	Nanocrystalline Twinning Induced Plasticity Steel with Superior Mechanical Properties Fabricated by Cold Rolling and Annealing. Materials Science Forum, 0, 753, 518-521.	0.3	1
116	Nitriding Effect on Corrosion Fatigue Strength of Low Alloy Steel in 1% HCl Aqueous Solution. Advanced Materials Research, 0, 891-892, 674-678.	0.3	0